

ChemComm

Chemical Communications

Accepted Manuscript

This article can be cited before page numbers have been issued, to do this please use: E. van der Pol, L. Krammer, J. Eder, D. Gross, R. C. Fischer, K. Miyamoto, R. Kourist and R. Breinbauer, *Chem. Commun.*, 2026, DOI: 10.1039/D6CC02837C.



This is an Accepted Manuscript, which has been through the Royal Society of Chemistry peer review process and has been accepted for publication.

Accepted Manuscripts are published online shortly after acceptance, before technical editing, formatting and proof reading. Using this free service, authors can make their results available to the community, in citable form, before we publish the edited article. We will replace this Accepted Manuscript with the edited and formatted Advance Article as soon as it is available.

You can find more information about Accepted Manuscripts in the [Information for Authors](#).

Please note that technical editing may introduce minor changes to the text and/or graphics, which may alter content. The journal's standard [Terms & Conditions](#) and the [Ethical guidelines](#) still apply. In no event shall the Royal Society of Chemistry be held responsible for any errors or omissions in this Accepted Manuscript or any consequences arising from the use of any information it contains.

COMMUNICATION

Hydrophobic pocket engineering of arylmalonate decarboxylase expands its substrate scope towards the synthesis of the (*R*)-enantiomers of sterically hindered carboxylic acids

Elske van der Pol,^{a,b} Lisa-Marie Krammer,^a Johannes Eder,^a Dominik Gross,^b Roland C. Fischer,^c Kenji Miyamoto,^d Rolf Breinbauer,^b Robert Kourist*^a

Received 00th January 20xx,
Accepted 00th January 20xx

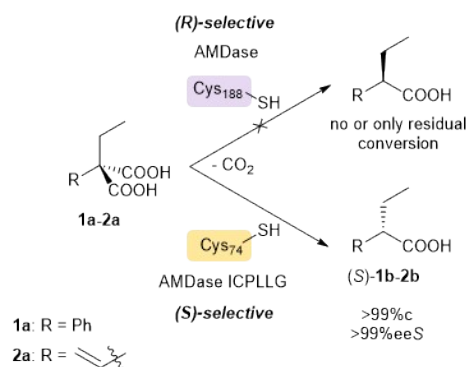
DOI: 10.1039/x0xx00000x

Arylmalonate decarboxylase (AMDase) stereoselectively converts disubstituted malonates to chiral carboxylic acids, but its substrate spectrum is very limited regarding the size of the smaller substituent. Inspired by the observation that (*S*)-selective AMDase variants also convert larger substrates, we unlocked the synthesis of the (*R*)-enantiomers of α -aryl and α -alkenyl *n*-butanoic acids and one *n*-pentanoic acid, respectively, in exquisite enantiopurity.

With their high selectivity and mild reaction conditions, enzymes have established themselves for the preparation of enantiomerically pure molecules.¹ Limitations of the substrate scope of enzymes are a challenge, which can be addressed by enzyme engineering.^{2,3} The synthesis of α -substituted carboxylic acids is a typical example of the complementary strengths of chemical and enzyme catalysis. Direct alkylation of arylacetic acids using chiral auxiliaries is practicable and widely used.^{4,5} Recently, direct stereoselective alkylation of arylacetic acids using chiral lithium amide as stereodirecting agent has been reported,⁶ giving access to a large number of α -alkyl carboxylic acids with enantiomeric excess ranging from 90–95%. A disadvantage is the requirement of the stoichiometric addition of an optically pure ligand. While the biocatalytic synthesis of α -chiral propanoic acids can be achieved by different enzyme classes in high to very high selectivity,^{7–13} there are only few examples on enzymes producing the corresponding optically pure α -substituted butanoic acids (Table S1).^{14–17} Asymmetric decarboxylation of prochiral α,α -disubstituted malonic acids by bacterial arylmalonate decarboxylase (AMDase) gives access to α -aryl and α -alkenyl alkanolic acid derivatives such as non-steroidal anti-inflammatory drugs (NSAIDs),^{18–22} α -heterocyclic propionic acids^{23,24} in high yield and excellent stereoselectivity.^{20,25} The stereoselectivity of the enzyme could be switched by

transplanting the catalytic Cys-residue to the opposite side of the substrate²⁶ and the activity of the resulting (*S*)-selective AMDase variant was improved by focused directed evolution,^{18,21,25,27} which has been explained by the formation of a second hydrophobic pocket in the active site.²⁸

A. Previous work



B. This work

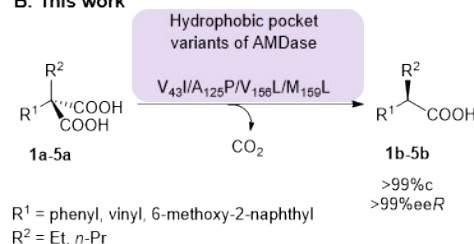


Fig. 1 A. Previous work: Engineered (*S*)-selective AMDase accepts α -ethyl substrates, while (*R*)-selective AMDase WT does not. B. This work: (*R*)-selective AMDase variants with an engineered hydrophobic pocket convert α -ethyl and *n*-propyl substrates.

AMDase accepts an impressive number of substrates having different larger substituents, with the only requirement that they should bear a delocalized π -electron system required for the stabilization of the nascent charge upon decarboxylation. In contrast, the acceptance of the second substituent is very restricted. AMDase accepts malonic acids with a hydrogen atom, a methyl, hydroxy, amine group, and halogen atoms.²⁹ In their study on the first purification of the enzyme, Ohta and Miyamoto reported that 2-ethyl-2-phenyl malonate (**1a**) was

^a Institute of Molecular Biotechnology, Graz University of Technology, Petersgasse 14, 8010 Graz, Austria.

^b Institute of Organic Chemistry, Graz University of Technology, Stremayrgasse 9, 8010 Graz, Austria.

^c Institute of Inorganic Chemistry, Graz University of Technology, Stremayrgasse 9, 8010, Graz, Austria.

^d Department of Biosciences and Informatics, Keio University, 3-14-1 Hiyoshi, Kohoku-ku, Yokohama 223-8522, Japan.



inert to the enzyme.³⁰ Recently, we could show that (*S*)-selective variants of AMDase having an extended hydrophobic pocket in the active site, such as AMDase V₄₃I/G₇₄C/A₁₂₅P/V₁₅₆L/M₁₅₉L/C₁₈₈G ('AMDase ICPLLG'), accepted malonic acids with a larger second substituent and decarboxylated 2-ethyl-2-vinyl malonate (**2a**) to 2-ethylbut-3-enoic acid (**2b**).³¹ The excellent enantiomeric purity (>99% ee) of the product demonstrated the outstanding capacity of AMDase to discriminate between the similarly sized ethyl and vinyl substituents.

In contrast, wildtype AMDase did not convert **2a** and showed only traces of **1b** after 20 h (Fig. 1A).³¹ On basis of this finding, we hypothesized that variants of the (*R*)-selective wildtype enzyme with an extended hydrophobic pocket could convert sterically hindered malonates with high stereoselectivity. Therefore, we prepared a series of α -aromatic and α -vinylic malonic acids with an ethyl and *n*-propyl group as second α -substituent (**1a-6a**) and investigated the activity and stereoselectivity of (*R*)-selective AMDase IPLL (V₄₃I/A₁₂₅P/V₁₅₆L/M₁₅₉L) with amino acid substitutions in the active site hydrophobic pocket (Fig. 2A). Our results confirm that the increased size and hydrophobicity of the active site lead to a wider substrate spectrum, thereby enabling access to optically pure α -aryl and α -alkenyl *n*-butanoic and *n*-pentanoic acids (Fig. 1B).

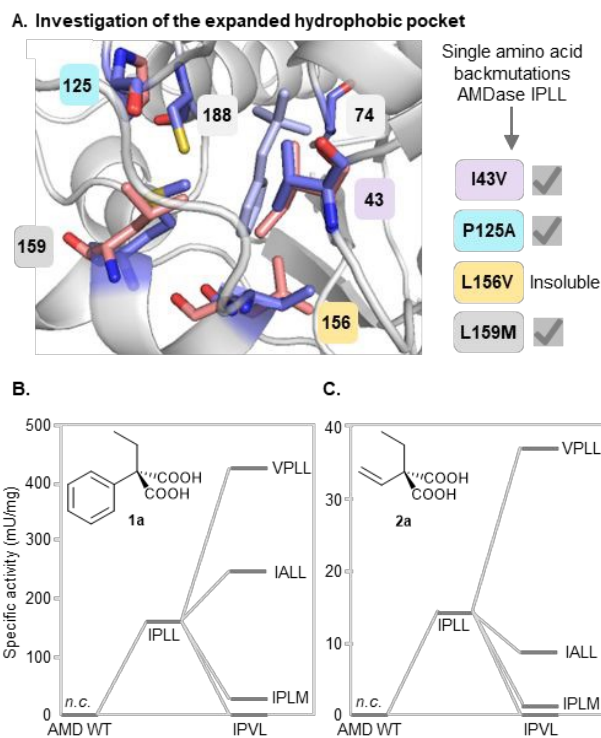
In (*R*)-selective AMDase (C188), the mutations I₄₃P₁₂₅L₁₅₆L₁₅₉ increase activity towards aromatic α -methyl malonates.^{21,25} We were pleased to find that AMDase I₄₃P₁₂₅L₁₅₆L₁₅₉ also showed full conversion with **1a** and **2a** (Fig. 2B,C), producing (*R*)-**1b** and (*R*)-**2b** in high optical purity (>98% ee). To test the effect of these single substitutions, I₄₃P₁₂₅L₁₅₆L₁₅₉ was back mutated by single-point mutations, resulting in four AMDase variants; AMDase V₄₃P₁₂₅L₁₅₆L₁₅₉, I₄₃A₁₂₅L₁₅₆L₁₅₉, I₄₃P₁₂₅V₁₅₆L₁₅₉, and I₄₃P₁₂₅L₁₅₆M₁₅₉ (Fig. 2A).

The amino acid substitution M₁₅₉L leads to higher activity towards α -methyl malonic acids (Fig. S1),^{25,27} therefore it is not surprising that I₄₃P₁₂₅L₁₅₆L₁₅₉ has also higher activity towards α -ethyl malonic acids than I₄₃P₁₂₅L₁₅₆M₁₅₉ (Fig. 2B,C). Unfortunately, soluble expression of AMD I₄₃P₁₂₅V₁₅₆L₁₅₉ was limited, and no specific activities could be measured for this variant. Reactions with cell-free extract demonstrated poor conversion. All soluble variants retained the activity towards α -methyl malonic acids and achieved full conversion with 2-methyl-2-phenyl malonic acid **7a** and 2-methyl-2-vinyl malonic acid **8a**, respectively (Fig. S21-S33).

Variant I₄₃A₁₂₅L₁₅₆L₁₅₉ has higher activity towards **1a** than I₄₃P₁₂₅L₁₅₆L₁₅₉, whereas activity towards **2a** was insignificantly lower, showing that the contribution of this substitution has only a minor effect. Surprisingly, back-mutation of I43 to valine (AMDase V₄₃P₁₂₅L₁₅₆L₁₅₉) further boosted the activity for both α -ethyl malonates (Fig. 2B,C), resulting in the fastest (*R*)-selective AMDase variant for the conversion of **2a** found so far (37.4 mU/mg, 2.7-fold improvement). In the liganded structure of AMDase G₇₄C/C₁₈₈S, the distance between the C β -atom of V43 and the C α -atom of the ligand phenyl acetate is only 5 Å. Substitution of isoleucine by the smaller valine residue, lacking

one methyl group, likely reduces steric congestion in this region and thereby facilitates more productive substrate positioning, resulting in enhanced reaction rates towards α -ethyl-malonates. Although A-values for methyl and ethyl are similar, van der Waals volumes increase substantially, indicating that flexible alkyl substituents may impose steric constraints.³²

Fig. 2 A. Active site of AMDase, with altered amino acids highlighted in purple (wildtype, PDB entry 3IP8) and light pink (IPLL variant). B. C. Specific activities of



designed AMDase variants with substrates **1a-2a**. AMDase IPVL produced a low level of soluble enzyme and was barely active. See Figure S3 for details, n=3.

The results of the backmutation show that the substitutions V₁₅₆L and M₁₅₉L contribute the strongest to the activity of I₄₃P₁₂₅L₁₅₆L₁₅₉. At position 43, L and V are possible, and at position 125, A and P. Not surprisingly, α -aromatic malonates react faster than α -vinylic (Fig. S1), which has been observed before^{25,31,33} and can be attributed to the increased capacity to stabilize the nascent negative charge during the course of the reaction. For AMDase I₄₃P₁₂₅L₁₅₆L₁₅₉ and the faster AMDase V₄₃P₁₂₅L₁₅₆L₁₅₉, the measured optical purities are shown in Table 1. For (*R*)-**1b**, excellent ee's were found for both variants, while for (*R*)-**2b**, reduced selectivity was observed. This is surprising as the (*S*)-selective AMDase ICPLLG discriminates well between the two substituents of **2a** (>99% ee). Back mutation of ICPLLG to AMDase VCPLLG resulted in a comparable positive trend in **2a** (Fig. S1). However, for **1a**, an adverse effect was observed. This can be rationalized by the altered binding mode of vinylic malonates compared to aryl malonates, in which the carboxylate is cleaved from the newly formed hydrophobic pocket.¹⁹ In this orientation, the residue at position 43 is part of the pocket accommodating the vinyl or ethyl substituent. Also, here, the substitution of isoleucine by the smaller valine residue reduces steric hindrance and allows for increasingly productive substrate positionings.



Table 1. Obtained enantiomeric excess (ee) of the chiral α -carboxylic acids produced by AMDase (on CFE), >99% conv. Aromatic acids **1b** were derivatized to the corresponding methyl esters (**Me-1b**) using TMS-diazomethane. Experiments were performed as triplicates. n.d. = not determined. *first eluting peak.

AMDase	(<i>R</i>)-Me- 1b	(<i>R</i>)- 2b	(+)- 3b	(<i>R</i>)- 4b	5b *
IPLL	>99% \pm 0.0	94% \pm 0.8	77% \pm 0.0	n.d.	n.d.
VPLL	>99% \pm 0.0	96% \pm 0.6	79% \pm 0.7	>99% \pm 0.0	>99% \pm 0.0

We then proceeded to investigate other substrates posing specific challenges for the enzyme. For the well-accepted α -ethyl substituted substrate **2a**, we observed a 100-fold lower activity for both (*R*)- and (*S*)-selective AMDases compared to α -methyl- α -vinyl malonate (**Fig. S1**), which might be caused by steric reasons. To investigate the effect of the additional rotational degree of freedom, we examined **3a** with bridged α -groups, limiting the free rotation of the alkyl side group (**Fig. 3A,B**). Due to the conformationally restricted cyclohexenyl ring of **3a**, it should be considered that the 2-cyclohexene malonate adopts a half-chair conformation with one carboxylate in pseudoaxial and one in pseudoequatorial position.³⁴ Typically, the axial substituents are energetically less favored due to unfavorable interactions/steric clashes with other axial substituents and/or the p-orbitals of the unsaturated carbon-carbon bond. Therefore, bond cleavage of the α -carbon and the pseudoaxial carbonyl carbon would be favored. Subsequently, cleavage of the carboxylate introduces a partial negative charge on the α -carbon in the transition state. In contrast to **2a**, where the vinyl group has free rotation, for **3a** the partial negative charge can be stabilized through hyperconjugation of the aligned C=C bond. Both the conformational restrictions and the stabilizing effect would favor the acceptance of **3a** over **2a**.

To investigate the impact of the G74C/C188G mutation on the specific activity, we determined the activity of the well-characterized (*R*)-selective AMDase IPLL and (*S*)-selective AMDase ICPLLG. For the AMDase IPLL, the rate for **3a** was similar to that for **2a** (approximately 15 mU/mg). In contrast, AMDase ICPLLG showed a 13-fold higher rate when comparing the strained malonate **3a** (133 mU/mg) to α -ethyl malonate **2a** (10 mU/mg) (**Fig. 3B**). Previously, an isotope labeling study combined by QM/MM metadynamics indicated that for alkenylic substrates, the cleaved carboxylate, the α -carbon, and the cysteine would ideally be aligned at a 180-degree angle. While movement of the α -substituents is restricted for **3a**, the reaction coordinates in AMDase IPLL are not aligned at the optimal 180-degree angle required for the borderline concerted mechanism of AMDase variants towards alkenylic substrates,³¹ which would clarify the similar rates observed for both substrates by AMDase IPLL.

In contrast, when **2a** and **3a** adopt the same binding mode as 2-methyl-2-vinyl malonate in AMDase ICPLLG, the α -carbon would be perfectly aligned at a 180-degree angle with the leaving carboxylate and C74. This binding mode allows the reaction to be borderline concerted, with the protonation by C74 being partially rate-limiting. The free rotation of the α -substituents, being hampered and not obstructing protonation,

further facilitates improved reactivity. Together, these effects might provide an explanation for the observed enhancement in the reaction rates obtained for **2a** and **3a** by AMDase ICPLLG (**Fig. 3B**). The stereoselectivity of the two (*R*)-selective AMDase variants towards **3a** was much lower than for **2a**. The small dialkyl malonates can bind in two inverse binding modes into the active site of AMDase, leading either to cleavage of the *pro-R* or the *pro-S* group, respectively.³¹ It can be easily imagined that due to the compact structure of **3a**, both binding modes have similar binding energies, making their discrimination very challenging.

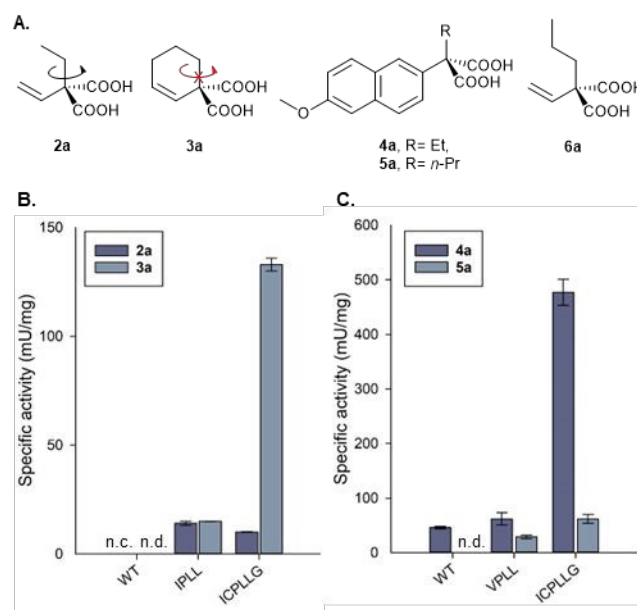


Fig. 3 A. Various α -alkenyl and (6-methoxy-2-naphthyl)-malonates. B. Specific activities of AMDase variants with **2a**, **3a**. AMD WT does not convert **2a** (n.c.). C. Specific activities of AMDase variants with **4a** and **5a**. The conversion of **3a** and **5a** by AMD WT is too low to determine its specific activities (n.d.).

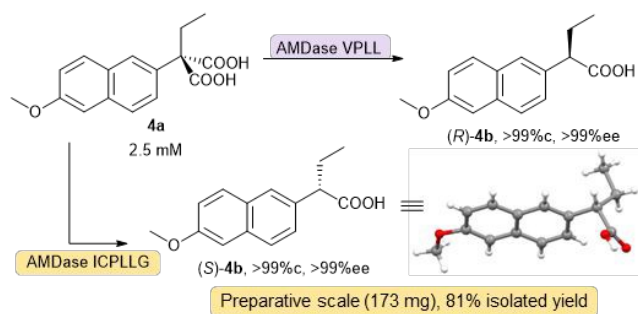
We then investigated the synthesis of both enantiomers of optically pure **4b**, which has recently been described as an effective aldo-keto reductase 1C3 inhibitor.³⁵ Variants VPLL (*R*) and ICPLLG (*S*) were chosen as they had shown the highest activity towards α -ethyl substituted malonates (**Fig. 3C and 4**). AMDase ICPLLG exhibited the highest specific activity toward **4a**, while AMDase VPLL showed a \sim 7-fold lower activity. Surprisingly, AMDase wildtype converted **4a**, albeit with 10-fold lower activity than AMDase VPLL. In comparison, the situation is reversed for the less sterically demanding naproxen malonate, which was converted 5-fold faster by the wildtype than by AMDase ICPLLG.¹⁸ This difference in the activity of wildtype and variants towards differently substituted α -aryl- α -ethyl substrates underlines that the effect of substitutions in the active site hydrophobic pocket of AMDase is hard to predict and highly substrate-specific.

Furthermore, we explored the acceptance of propyl-(6-methoxy-2-naphthyl) (**5a**) and 2-propyl-2-vinyl malonate (**6a**). AMDase ICPLLG and VPLL indicated good acceptance of **5a** (**Fig. 3C**), leading to 99% conversion. Yet the vinyl compound demonstrated only limited conversion (39% and 19% for



AMDase ICPLLG and VPLL, respectively, **Table S11**). We attribute this to the less effective stabilization of the evolving negative charge by the vinylic compound, combined with the steric hindrance of the *n*-propyl substituent. For the AMDase variants VPLL and ICPLLG, the specific activities toward **5a** were determined (**Fig. 3C**). Both variants exhibited markedly reduced rates for **5a** compared to those for **4a**, consistent with increased steric hindrance and greater rotational freedom of the *n*-propyl group. Overall, the engineered hydrophobic pocket of the variants ICPLLG and VPLL helps to overcome the limitations of the wildtype.

Fig. 4. Conversion of **4a** by AMDase VPLL and ICPLLG. (*S*)-**4b** was produced on a



preparative scale using (*S*)-selective AMDase ICPLLG.

Both engineered AMDase variants were able to convert **4a** and **5a** with excellent enantioselectivity (>99% ee) (**Table 1**, **Fig. S36**, **S39**), thereby providing access to both enantiomers of the aldoketo reductase 1C3 inhibitor **4b**. Recently, Adeniji and coworkers obtained the effective chiral acid **4b** by synthesizing the racemate, followed by chiral HPLC separation.³⁵ Since AMDase ICPLLG and VPLL demonstrated the ability to produce the chiral acid in high purity, an enzymatic step in the synthesis process could be advantageous and increase the theoretical yield from 50% to 100%. With two stereocomplementary enzymes in hand, we wanted to demonstrate their scale-up potential. Using the more active (*S*)-producing enzyme, we synthesized (*S*)-**4b**. The biotransformation with AMDase ICPLLG using 173 mg of **4a** produced (*S*)-**4b** (**Fig. 4**) in 81% isolated yield. We confirmed the absolute stereochemical configuration of **4b** obtained by AMDase ICPLLG-catalyzed decarboxylation *via* X-ray crystallography.

In conclusion, variation of active-site residues of AMDase, particularly the substitutions V₁₅₆L and M₁₅₉L, unlocked activity towards disubstituted malonic acids with an α -substituent larger than a methyl group. While wildtype decarboxylase has no or only very low activity towards these substrates, AMDase IPLL and variants thereof showed full conversion, enabling the enzymatic synthesis of α -aryl and α -alkenyl *n*-butanoic acids and one example for an *n*-pentanoic acid with very high stereoselectivity. It should be noted that point mutations in the hydrophobic pocket exert a strong and very substrate-specific effect on the conversion of these sterically hindered substrates, making it worth to investigate small sets of variants instead of a single AMDase variant for the conversion of sterically hindered malonic acids.

Author contributions

View Article Online

DOI: 10.1039/D6CC02837C

E.v.d.P. conceptualized, coordinated, performed experiments, visualized, and prepared the manuscript. L.M.K. performed and analyzed the experiments with the naproxen malonates. She also prepared a part of the manuscript. J.E. generated the back-mutated AMDase variants and performed initial studies. D.G. performed the work-up and product purification of the preparative scale biocatalysis reactions, and the crystallization. R.C.F. performed the X-ray diffraction and structure refinement. K.M. conceptualized and participated in discussions leading to the design of this study. R.B. conceptualized, provided funding, supervised, and prepared the manuscript. R.K. conceptualized, provided funding, supervised, visualized, and prepared the manuscript. All authors contributed to the data interpretation, reviewed, and approved the manuscript.

Conflicts of interest

There are no conflicts to declare.

Acknowledgements

This research was funded in part by the Austrian Science Fund (FWF) (Funding DOI: 10.55776/P34280) For open access purposes, the author has applied a CC BY public copyright license to any author accepted manuscript version arising from this submission. We gratefully acknowledge financial support by NAWI Graz.

Data availability

Experimental details, sequences, NMR spectra, (chiral) GC & HPLC chromatograms are available in the Supporting Information. Deposition Number 2545010 contains the supplementary crystallographic data for this paper. These data can be obtained free of charge via the joint Cambridge Crystallographic Data Centre (CCDC) and Fachinformationszentrum Karlsruhe Access Structures service.

Notes and references

- R. Buller, S. Lutz, R. J. Kazlauskas, R. Snajdrova, J. C. Moore, U. T. Bornscheuer, *Science*, 2023, **382**, 6673.
- C. K. Savile, J. M. Janey, E. C. Mundorff, J. C. Moore, S. Tam, W. R. Jarvis, J. C. Colbeck, A. Krebber, F. J. Fleitz, J. Brands, P. N. Devine, G. W. Huisman, G. J. Hughes, *Science*, 2010, **329**, 305–309.
- K. K. F. Bauer, S. Vaupel, E. Vos, A. Wanz, D. Kracher, T. Schöngassner, L.-E. Meyer, J. Gay, S. C. L. Kamerlin, S. Kara, R. Kourist, *preprint*, 2025, <https://doi.org/10.26434/chemrxiv-2025-frgxt>.
- A. G. Myers, B. H. Yang, H. Chen, L. McKinstry, D. J. Kopecky, J. L. Gleason, *J. Am. Chem. Soc.* 1997, **119**, 6496–6511.
- D. A. Evans, M. D. Ennis, D. J. Mathre, *J. Am. Chem. Soc.* 1982, **104**, 1737–1739.
- C. E. Stivala, A. Zakarian, *J. Am. Chem. Soc.* 2011, **133**, 11936–11939.



- 7 L. Steenkamp, D. Brady, *Process Biochemistry*, 2008, **43**, 1419–1426.
- 8 J. P. S. Choo, F. L. Sirota, W. W. L. See, B. Eisenhaber, Z. Li, *ACS Catal.* 2023, **13**, 11268–11276.
- 9 J. A. Friest, Y. Maezato, S. Broussy, P. Blum, D. B. Berkowitz, *J. Am. Chem. Soc.* 2010, **132**, 5930–5931.
- 10 P. Galletti, E. Emer, G. Gucciardo, A. Quintavalla, M. Pori, D. Giacomini, *Org. Biomol. Chem.* 2010, **8**, 4117–4123.
- 11 W. W. L. See, X. Li, Z. Li, *Adv. Synth. Catal.* 2023, **365**, 68–77.
- 12 D.-I. Kato, K. Teruya, H. Yoshida, M. Takeo, S. Negoro, H. Ohta, *The FEBS Journal*, 2007, **274**, 3877–3885.
- 13 P. Könst, H. Merckens, S. Kara, S. Kochius, A. Vogel, R. Zuhse, D. Holtmann, I. W. C. E. Arends, F. Hollmann, *Angew. Chem. Int. Ed.* 2012, **51**, 9914–9917.
- 14 M. Pickl, R. Marín-Valls, J. Joglar, J. Bujons, P. Clapés, *Adv. Synth. Catal.* 2021, **363**, 2866–2876.
- 15 E. Fernández-Álvarez, R. Kourist, J. Winter, D. Böttcher, K. Liebeton, C. Naumer, J. Eck, C. Leggewie, K.-E. Jaeger, W. Streit, U. T. Bornscheuer, *Microbial Biotechnology*, 2010, **3**, 59–64.
- 16 K. Engström, J. Nyhlén, A. G. Sandström, J.-E. Bäckvall, *J. Am. Chem. Soc.* 2010, **132**, 7038–7042.
- 17 D. Torri, L. Bering, L. R. L. Yates, S. M. Angiolini, G. Xu, S. Cuesta-Hoyos, S. A. Shepherd, J. Micklefield, *Angew. Chem. Int. Ed.* 2025, **64**, e202422185.
- 18 S. Yoshida, J. Enoki, R. Kourist, K. Miyamoto, *Biosci. Biotechnol. Biochem.* 2015, **79**, 1965–1971.
- 19 J. Enoki, C. Mügge, D. Tischler, K. Miyamoto, R. Kourist, *Chem.–Eur. J.* 2019, **25**, 5071–5076.
- 20 J. Enoki, M. Linhorst, F. Busch, Á. G. Baraibar, K. Miyamoto, R. Kourist, C. Mügge, *Mol. Catal.* 2019, **467**, 135–142.
- 21 S. K. Gaßmeyer, J. Wetzig, C. Mügge, M. Assmann, J. Enoki, L. Hilterhaus, R. Zuhse, K. Miyamoto, A. Liese, R. Kourist, *ChemCatChem*, 2016, **8**, 916–921.
- 22 M. Aßmann, A. Stöbener, C. Mügge, S. K. Gaßmeyer, L. Hilterhaus, R. Kourist, A. Liese, S. Kara, *React. Chem. Eng.* 2017, **2**, 531–540.
- 23 R. Lewin, M. Goodall, M. L. Thompson, J. Leigh, M. Breuer, K. Baldenius, J. Micklefield, *Chem.–Eur. J.* 2015, **21**, 6557–6563.
- 24 C. A. Blakemore, S. P. France, L. Samp, D. M. Nason, E. Yang, R. M. Howard, K. J. Coffman, Q. Yang, A. C. Smith, E. Evrard, W. Li, L. Dai, L. Yang, Z. Chen, Q. Zhang, F. He, J. Zhang, *Org. Process Res. Dev.* 2021, **25**, 421–426.
- 25 K. Okrasa, C. Levy, M. Wilding, M. Goodall, N. Baudendistel, B. Hauer, D. Leys, J. Micklefield, *Angew. Chem. Int. Ed.* 2009, **121**, 7827–7830.
- 26 Y. Ijima, K. Matoishi, Y. Terao, N. Doi, H. Yanagawa, H. Ohta, *Chem. Commun.* 2005, **7**, 877–879.
- 27 Y. Miyauchi, R. Kourist, D. Uemura, K. Miyamoto, *Chem. Commun.* 2011, **47**, 7503–7505.
- 28 M. Biler, R. M. Crean, A. K. Schweiger, R. Kourist, S. C. L. Kamerlin, *J. Am. Chem. Soc.* 2020, **142**, 20216–20231.
- 29 K. Miyamoto, R. Kourist, *Appl. Microbiol. Biotechnol.* 2016, **100**, 8621–8631.
- 30 K. Miyamoto, H. Ohta, *Eur. J. Biochem.* 1992, **210**, 475–481.
- 31 E. van der Pol, T. Schlatzer, G. Hoffka, B. Di Geronimo, J. Eder, A. K. Schweiger, M. Karava, D. Gross, R. C. Fischer, D. Kracher, R. Kazlauskas, K. Miyamoto, S. C. L. Kamerlin, R. Breinbauer, R. Kourist, *J. Am. Chem. Soc.* 2025, **147**, 39271–39283.
- 32 E. L. Eliel and S. H. Wilen, *Stereochemistry of Organic Compounds*, Wiley-VCH, 1994.
- 33 M. E. S. Lind, F. Himo, *ACS Catal.* 2014, **4**, 4153–4160.
- 34 J. Clayden, N. Greeves and S. Warren, *Organic Chemistry*, Oxford University Press: Oxford, New York, 2012.
- 35 A. Adeniji, M. J. Uddin, T. Zang, D. Tamae, P. Wangtrakuldee, L. J. Marnett, T. M. Penning, *J. Med. Chem.* 2016, **59**, 7431–7444.

View Article Online
DOI: 10.1039/D6CC02837C



Data availability statement

View Article Online
DOI: 10.1039/D6CC02837C

Experimental details, sequences, NMR spectra, (chiral) GC & HPLC chromatograms are available in the Supporting Information. Deposition Number 2545010 contains the supplementary crystallographic data for this paper. These data can be obtained free of charge via the joint Cambridge Crystallographic Data Centre (CCDC) and Fachinformationszentrum Karlsruhe Access Structures service

Robert Kourist (on behalf of all authors)

